

Check for updates

Integrated Transcriptome Analysis of Radioresistant Cells Revealed Genes and Pathways Predictive Of Tumor Response to Radiotherapy and Chemotherapy in Breast Cancer

Isidro X. Perez-Añorve, Mauricio Flores-Fortis, Carlos C. Patiño-Morales, Elizabeth Ortiz-Gutierrez, Oscar Del Moral-Hernandez, Claudia H. Gonzalez-De la Rosa, Ernesto Soto-Reyes, Raul Bonilla-Moreno, Margarita Chavez Saldaña, Daniel A. Landero-Huerta, Daniel Ortega-Bernal, Nicolas Villegas, and Elena Arechaga-Ocampo*

Breast cancer cells exposed to radiotherapy frequently develop radiation resistance through molecular and phenotypic changes. While there is evidences of pathways controlling radioresistance, the evolution of diverse cell phenotypes and transcriptional changes as mediators of radioresistance in breast cancer are restricted. Moreover, the effectiveness of the chemotherapy on radioresistant cells remains uncertain. In this work, an isogenic model of radioresistant breast cancer cells (RR cells) is used to study this phenotype. RR cells show high survival rates after radiation, moreover, RR cells of the triple negative breast cancer (TNBC) subtype show a significantly advanced invasiveness phenotype. Notably, RR cells are significantly sensitive to chemotherapy by inhibit cell survival and promote apoptosis. Transcriptomics and gene co-expression network analysis identify differentially expressed genes (DEGs) and hub genes related to survival and apoptosis pathways in the RR cells of luminal subtype, while in TNBC subtype, cell migration, cell differentiation, and immune pathways are enriched. Hub genes predict the failure of radiotherapy in breast cancer patients, but they are also related to pathological complete response after chemotherapy. Transcriptome changes during acquired radioresistance uncover genes and pathways associated to radio and chemotherapy response. These results demonstrate that radioresistant pathways may converge to develop collateral chemo-sensitivity.

1. Introduction

Radiotherapy is used in multimodal treatment approaches for breast cancer and has been shown to be effective in reducing recurrence and mortality rates.[1,2] However, some patients show treatment failure due to radioresistant cells, which are partially responsible for progression and relapse of the disease.[3-6] Genetics and epigenetics heterogeneity in breast cancer tumors implies that a fraction of cells in the tumors may present innate radioresistance. Over the course of the treatment, some breast cancer cells evade the cytotoxic effect of radiation acquiring survival capabilities and developing radioresistance.[7] The molecular mechanism involved in the adaptive response to radiotherapy have been widely reported, genetic and epigenetic aberrations, failures in cell death pathways, inhibition of tumor suppressors genes, gain of function of oncogenes, deregulation of transcriptional factors and over-activation of cell proliferation and survival pathways underlying radioresistance in breast cancer.[4-6,8-10]

I. X. Perez-Añorve Laboratorio de Patologia Vascular Cerebral Instituto Nacional de Neurologia y Neurocirugia Manuel Velasco Suarez Mexico City 14269, Mexico



© 2024 The Author(s). Advanced Therapeutics published by Wiley-VCH GmbH. This is an open access article under the terms of the Creative Commons Attribution-NonCommercial-NoDerivs License, which permits use and distribution in any medium, provided the original work is properly cited, the use is non-commercial and no modifications or adaptations are made.

DOI: 10.1002/adtp.202300274

I. X. Perez-Añorve, C. C. Patiño-Morales, C. H. Gonzalez-De la Rosa, E. Soto-Reyes, D. Ortega-Bernal, E. Arechaga-Ocampo Departamento de Ciencias Naturales, Unidad Cuajimalpa

Universidad Autonoma Metropolitana Mexico City 05348, Mexico

E-mail: earechaga@cua.uam.mx

M. Flores-Fortis

Posgrado en Ciencias Naturales e Ingenieria, Unidad Cuajimalpa Universidad Autonoma Metropolitana

Mexico City 05348, Mexico

C. C. Patiño-Morales

Laboratorio de Biologia del Desarrollo y Teratogenesis Experimental Hospital Infantil de Mexico "Federico Gomez"

Mexico City 06720, Mexico

www.advtherap.com

All these mechanisms have also been reported in the tumor evolution of breast cancer after other treatment modalities, including chemotherapy.[11] Silencing of the EGF/EGFR pathway supports sensitivity to radiation, making it the preferred therapeutic target in breast cancer and other neoplasms. [12,13] Likewise, JAK/STAT and interferon/STAT1 pathways promote cell resistance to therapies that cause genotoxic damage such as radiation and some chemotherapeutic agents.[14] In contrast, STAT1 overexpression is related to a better response to immunological therapies based on PD-L1.[15] Some components of the inflammatory response, such as TNF pathways, increased radioresistance, through activation of transcription factors as NF- κ B resulting in the modulation of genes implicate in anti-apoptosis, proliferation, and cell cycle. [4] Although the role of these genes in conjunction with other molecular components to promote therapeutic resistance cells have been experimentally demonstrated,[16] their role in cells with acquired radioresistance exposed to chemotherapies is still unexplored.[8,9]

Radioresistant luminal MCF-7 (MCF-7RR) and TNBC MDA-MB-231 (MDA-MB-231RR) cells were experimentally established after fractionated radiotherapy frequently implemented as a standard radiotherapy scheme in breast cancer.[17] The survival ability of the RR cells has been experimentally demonstrated, but the underlying radioresistance mechanism and the implication in the effectiveness of the other therapies as anticancer drugs remains uncertain because of the limited amount of experimental data. To study the behavior of RR cells in response to chemotherapy, we exposed RR cells to chemotherapy agents commonly used in breast cancer treatment. Moreover, we investigated the transcriptional changes and co-expression gene networks of the RR cells to identify genes and biological pathways related to resistance to radiotherapy and the chemotherapy response.

In this work, we provide evidence of chemo-sensitive phenotype of radioresistant breast cancer cells. The evaluation of the global changes of gene expression evidenced DEGs related to survival and apoptosis pathways in radioresistant luminal breast cancer cells, while migration, cell differentiation, and immune response were enriched in radioresistant TNBC. Together, these results showed that increased expression of the EGFR, STAT1, TNF, GB2L1, SRC, and MAPK1 genes were worse prognostic factors for RFS in breast cancer patients undergoing radiation therapy; however, they were also associated with a complete patho-

E. Ortiz-Gutierrez

Programa Investigadoras e Investigadores por México Coordinacion de Repositorios, Investigacion y Prospectiva (CRIP), Consejo Nacional de Ciencia y Tecnologia (CONACYT) Mexico City 03940, Mexico

O. Del Moral-Hernandez

Laboratorio de Virologia, Facultad de Ciencias Quimico Biologicas Universidad Autonoma de Guerrero Chilpancingo 39070, Mexico

R. Bonilla-Moreno, N. Villegas

Departamento de Biomedicina Molecular Centro de Investigacion y de Estudios Avanzados (CINVESTAV) Mexico City 07360, Mexico

M. Chavez Saldaña, D. A. Landero-Huerta Laboratorio de Biologia de la Reproduccion Instituto Nacional de Pediatria Mexico City 04530, Mexico

logical response after chemotherapy. This study may provide precise understanding of mechanisms contributing to cell radioresistance and response to chemotherapy to reconsider the multimodal treatment approaches for breast cancer.

2. Results

2.1. Radioresistant Breast Cancer Cells Display Sensitivity to Doxorubicin, Cyclophosphamide, Docetaxel, and Cisplatin

MCF-7RR and MDA-MB-231RR cells were previously established by exposed parental cells to hypo-fractionated radiation (Figure 1A).[17] Cell invasion, proliferation, and survival were assessed to evaluate the phenotypic characteristics of RR cells. Invasion analyses indicated no changes in invasiveness of MCF-7RR cells (Figure 1B), however, invasiveness of MDA-MB-231RR cells was significantly increased compared to parental controls (Figure 1C). Cell radioresistance was demonstrated by cell proliferation and survival assays MCF-7RR (Figure 1D,F) and MDA-MB-231RR (Figure 1E,G) cells showed higher cell proliferation and survival rates than parental cells after ionizing radiation, corroborating the radioresistant-phenotype. In addition, parental and RR cells were exposed to increased doses of doxorubicin cyclophosphamide and docetaxel to assess chemo-responses by determinate survival and apoptosis rates. MCF-7RR cells (Figure 2A) and MDA-MB-231RR cells (Figure 2B) showed significantly low viability when they were exposure to doxorubicin, cyclophosphamide, and docetaxel compared to parental cells. In the apoptosis assays, the results showed that MCF-7RR cells showed significantly higher levels of apoptosis in response to lethal doses of doxorubicin, cyclophosphamide, and docetaxel compared to parental cells (Figure 2C); however, apoptosis levels in response to cisplatin (used as positive control) did not show differences. These results were according to cytotoxic assays. On the other hand, MDA-MB-231 and MDA-MB-231RR cells (Figure 2D) showed greater evasion of apoptosis induced by doxorubicin, cyclophosphamide, and docetaxel compared to MCF-7 and MCF-7RR cells (Figure 2C), suggesting that luminal breast cancer cells could favor chemo-sensitivity more than TNBC cells. Besides, MDA-MB-231RR cells were more sensitive to apoptosis induced by doxorubicin, cyclophosphamide, and cisplatin than parental cells. These results were consistent with cytotoxicity results. However, MDA-MB-231RR cells showed low levels of apoptosis than parental cells (Figure 2D). These results were opposing to the cytotoxicity results (Figure 2B); suggesting that docetaxel might induce other kind of cell death than apoptosis. These results suggest that acquired radioresistance could favor pathways associated to chemo-sensitivity, mainly promotes apoptosis.

2.2. Transcriptomic Landscape of Radioresistant Breast **Cancer Cells**

To explore changes in the global expression of genes related to radioresistance, the DEGs were identified in MCF-7RR and MDA-MB-231RR cells compared to parental MCF-7 and MDA-MB-231 cells. In MCF-7RR cells were identified 151 DEGs (Table S1, Supporting Information), including 81 genes up-regulated and 70 genes repressed. Volcano plot and hierarchical clustering CIENCE NEWS

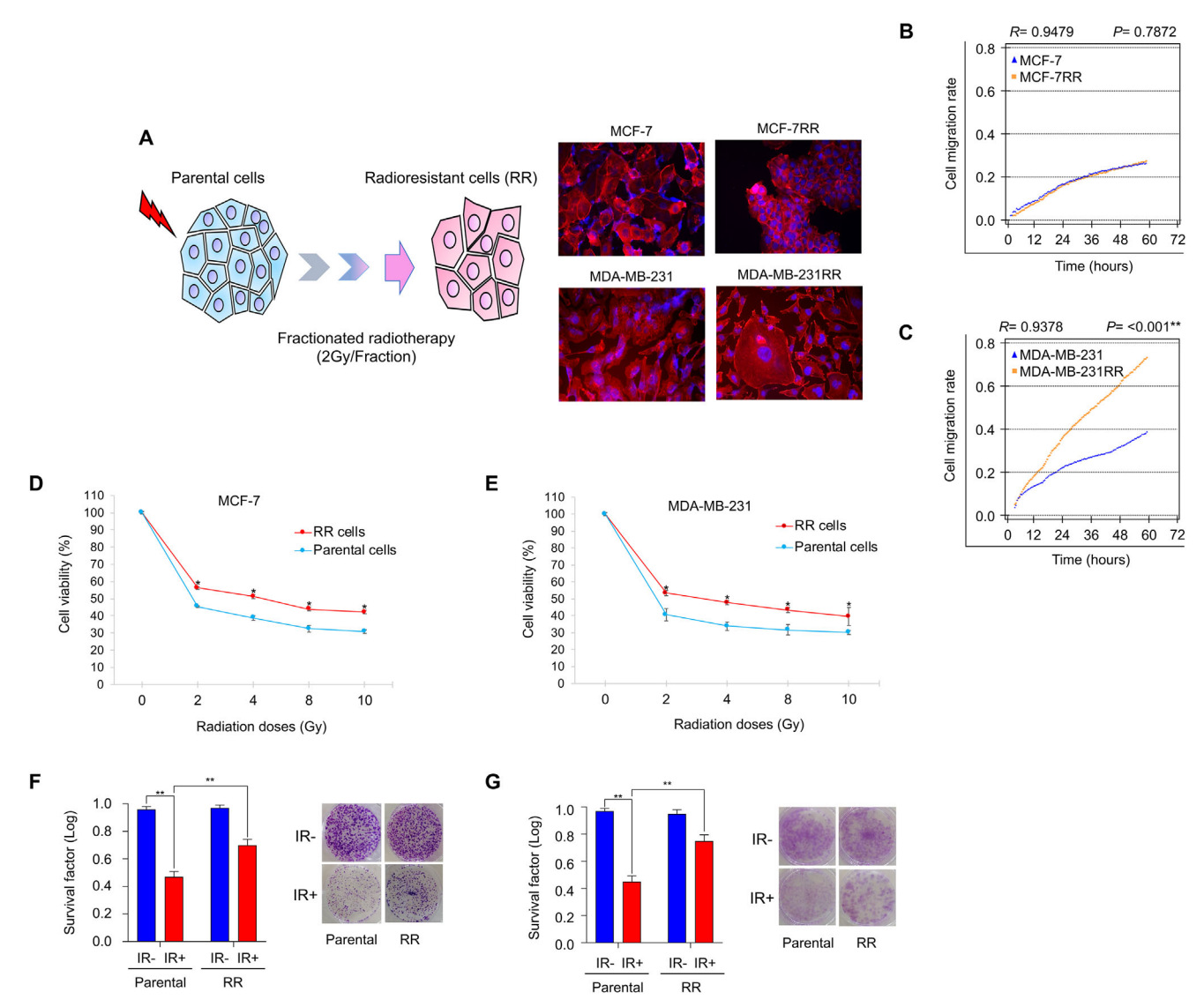


Figure 1. Radioresistant breast cancer cells show survival advantages to radiation. A) Establishment of radioresistant breast cancer cells. Parental MCF-7 and MDA-MB-231 cells were submitted to fractioned irradiation method using 2 Gy of ionizing radiation to reach total dose of 30 Gy, resulting in the MCF-7RR and MDA-MB-231RR cell lines. Representative images of the morphology of parental and radioresistant cells by fluorescence microscopy. Migration of B) MCF-7RR and C) MDA-MB-231RR cells. Migration cells were monitored for 72 h. Radioresistance of MCF-7RR and MDA-MB-231RR cells was confirmed by MTT assays D,E) after growing doses of irradiation, and clonogenic assays F,G) after 4 Gy of irradiation. The SF of irradiated (IR+) MCF-7RR and MDA-MB-231RR cells was normalized by the SF of non-irradiated (IR-) cells. Representative images of the results of the clonogenic assays are shown. Error bar, SD from three independent experiments. Error bar indicates the SD from three independent experiments. *****p < 0.001, ****p < 0.001, ***p < 0.001; *p < 0.005 by Student's t-test.

of DEGs are graphically shown (**Figure 3A**,**B**). Gene ontology (GO) and pathway enrichment analysis showed that DEGs were enriched in pathways related to response to drugs, apoptosis, cell proliferation and response to radiation (Figure 3C). Highlighted up-regulated genes as *BCL2*, *CTSH*, *ITGB6*, *PLD1*, *and ADM* and down-regulated genes as *ERBB4*, *CAV1*, *CAV2*, *DKK1*, *ITGA6*, and *SOX2* which were enrichment in drug response processes, negative apoptosis regulation, cell migration and the Wnt pathway (Table S2, Supporting Information).

The transcriptome analysis of MDA-MB-231RR cells revealed 150 DEGs (Table \$3, Supporting Information), of which 88 were

up-regulated and 62 were suppressed. Volcano plot and hierarchical clustering of DEGs are graphically shown (Figure 3D,E). According to GO and pathway enrichment analysis, DEGs in MDA-MB-231RR cells are involved in significant process of signal transduction, immune response, cell adhesion, transcription regulation, inflammatory response, DNA methylation, angiogenesis, and gamma radiation response (Figure 3F). Particularly, the up-regulated genes as CCL4, IRAK3, IL1B, C5, and EGR1, and their counterpart repressed genes such as CCL20, CXCL10, CCL5, OASL, IL7R, and KDM1B were found significantly enriched in signal transduction pathways, immune

2363987, 2024, 7, Downloaded from https://advanced.onlinelibrary.wiley.com/doi/10.1002/adtp.202300274 by Universidad Autonoma Metropolitana, Wiley Online Library on [11/08/2025]. See the Terms and Conditions

and-conditions) on Wiley Online Library for rules of use; OA articles are governed by the applicable Creative Commons

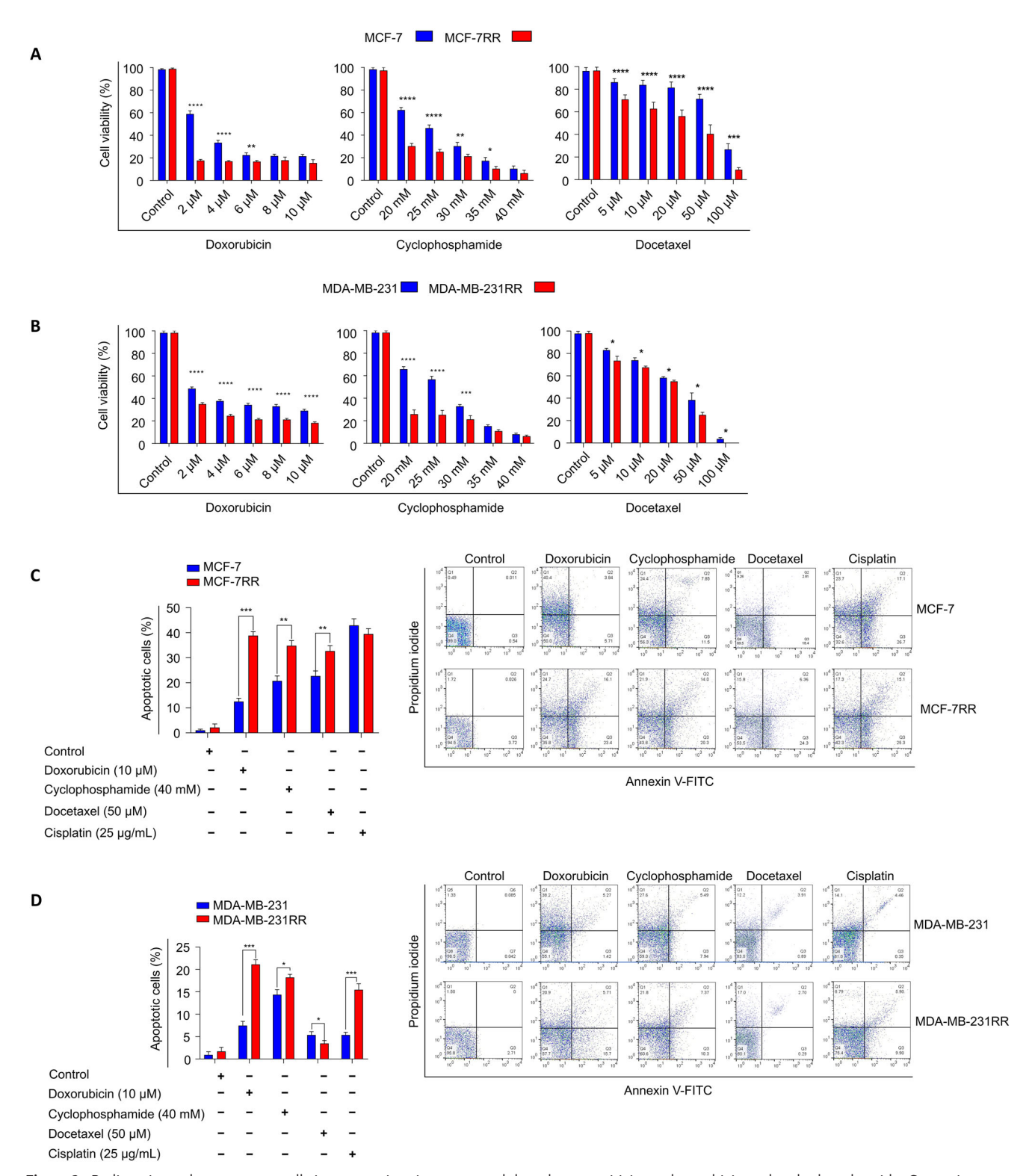


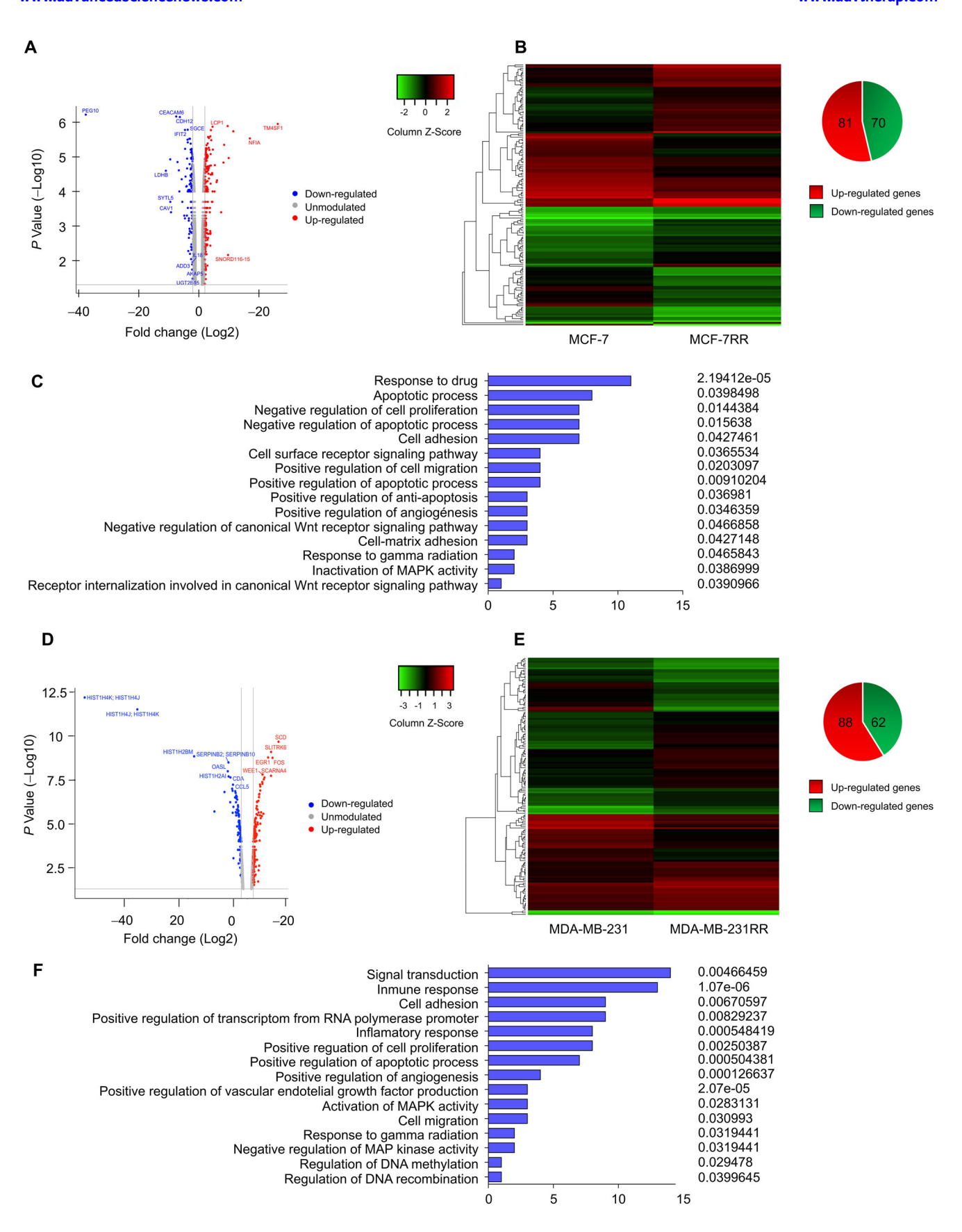
Figure 2. Radioresistant breast cancer cells improve migration rates, and they show sensitivity to doxorubicin and cyclophosphamide. Cytotoxic assays of parental and radioresistant A) MCF-7 cells and B) MDA-MB-231 cells after 24 h of exposure to increasing doses of doxorubicin, cyclophosphamide, and docetaxel. Apoptosis was measured by Annexin-V-FITC assays. Parental and radioresistant C) MCF-7 and D) MDA-MB-231 cells were exposed for 24 h to lethal doses of doxorubicin (10 μM), cyclophosphamide (40 mM), docetaxel (50 μM), and cisplatin (25 μg/mL) as positive control of cell deathinducing agent. Graphical representation of the results of Annexin-V-FITC assays show the cells treated with chemotherapeutic agents (+) compared with non-treated cells (-). Representative images of flow cytometry results are shown. Error bar indicates the SD from three independent experiments. p < 0.0001, *** p < 0.001, **p < 0.01; *p < 0.05 by Student's t-test.

23663987, 2024, 7, Downloaded from https://advanced

onlinelibrary.wiley.com/doi/10.1002/adtp.202300274 by Universi-

Metropolitana, Wiley Online Library on [11/08/2025]. See the Terms

on Wiley Online Library for rules of use; OA articles are governed by the applicable Creative Commons



23663987, 2024, 7, Downloaded from https://advanced.onlinelibrary.wiley.com/doi/10.1002/adtp.202300274 by Universidad Autonoma Metropolitana, Wiley Online Library on [11/08/2025]. See the Terms

und-conditions) on Wiley Online Library for rules of use; OA articles are governed by the applicable Creative Commons

www.advtherap.com

Figure 3. Transcriptome landscape of MCF-7RR and MDA-MB-231RR cells. Volcano plots show the dispersion of the DEGs in A) MCF-7RR and D) MDA-MB-231RR cells, faced the magnitude of change (Fold change Log2) and statistical significance (P value). Blue color indicates down-regulated genes and red indicates up-regulated genes. Heat map show the differential expression display of DEGs in MCF-7RR B) and MDA-MB-231RR E) cells. The pie chart indicates up-regulated (red) and down-regulated (green) genes. Graphs showing GO, signaling pathways and biological processes of the DEGs in C) MCF-7RR and F) MDA-MB-231RR cells.

response, vascular growth, angiogenesis, recombination and DNA methylation (Table S2, Supporting Information).

2.3. Genes Co-Expression Analysis Identify Hub Genes Associated to Radiotherapy Response

Gene co-expression networks from transcriptome data were constructed to identify genes with similar expression patterns and highly correlate to collective functions. Samples from radioresistant and parental cells clustered and visualized in the heatmaps were used to define the relationship between phenotype and sample dendrogram (Figure S1A,B, Supporting Information). Using the dynamic tree-cutting algorithm, genes were grouped into 4 modules for MCF-7RR cells (Figure 4A) and 12 mod-

ules for MDA-MB-231RR cells (**Figure 5A**). Brown modules of MCF-7RR cells (7490 genes) and MDA-MB-231RR cells (3985 genes) were significantly associated with radioresistant phenotype (Figure S1C–F, Supporting Information). The eigengene distribution was hierarchical clustering to determine the degree of deregulation of the modules. Overall, 190 genes were upregulated and 159 genes were down-regulated in the module brown of MCF-7RR cells compared to parental cells (Figure 4B; Table S4, Supporting Information). While 239 and 186 genes were up- and down-regulated respectively in the brown module of MDA-MB-231RR cells compared to parental cells (Figure 5B; Table S5, Supporting Information).

Genes from the brown module of the MCF-7RR cells were enriched in metabolic processes, negative regulation of humoral immune response, mitotic processes, and DNA repair.

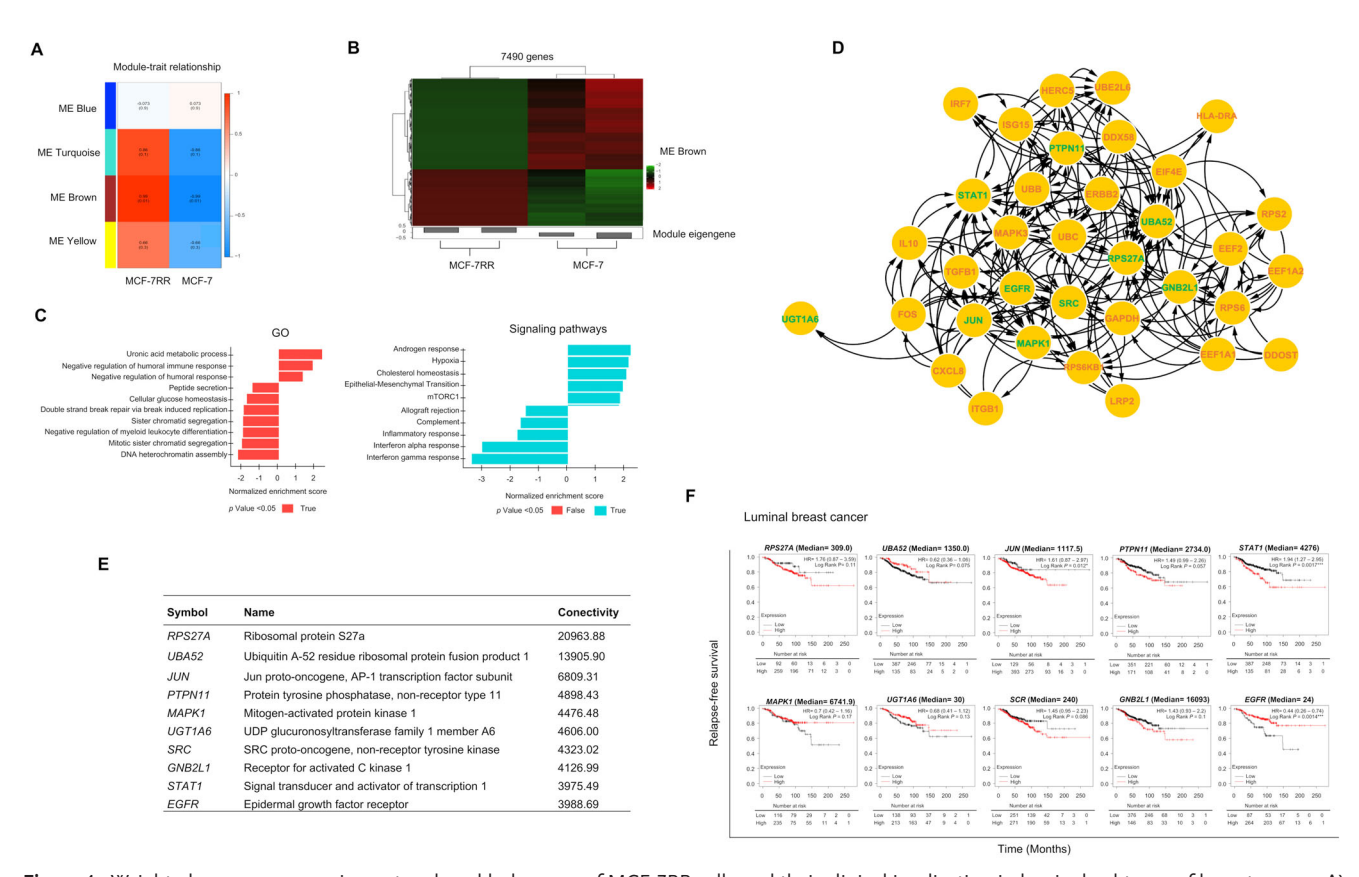


Figure 4. Weighted gene co-expression network and hub genes of MCF-7RR cells and their clinical implication in luminal subtypes of breast cancer. A) Correlation between the gene modules of the transcriptome of MCF-7RR cells. The connectivity of eigengenes analysis grouped into 4 modules is shown. B) Heat map that represents the correlation of 7490 genes of the brown module associated to radioresistant phenotype. Bar plots of gene set enrichment analysis for C) GO and enrichment signaling pathways of the brown module genes of MCF-7RR cells. D) Interactome showing the top 10 hub genes and the co-expression network with 37 nodes. Gene names in green indicate the top 10 hub genes in the subnetwork based on the betweenness score. E) Table betweenness score of hub gene with higher degrees of connectivity from brown module of MCF-7RR. F) Kaplan-Meier curves of RFS related to high versus low expression of hub genes in patients diagnosed with luminal breast cancer treated with radiotherapy. High or low expression levels according to > median or \leq median expression levels of each gene. Curves were compared using a log-rank test $^*p \leq 0.05$; $^{**}p \leq 0.01$, $^{***}p \leq 0.001$. Rpm, reads per million.

and-conditions) on Wiley Online Library for rules of use; OA articles are governed by the applicable Creative Commons

www.advtherap.com

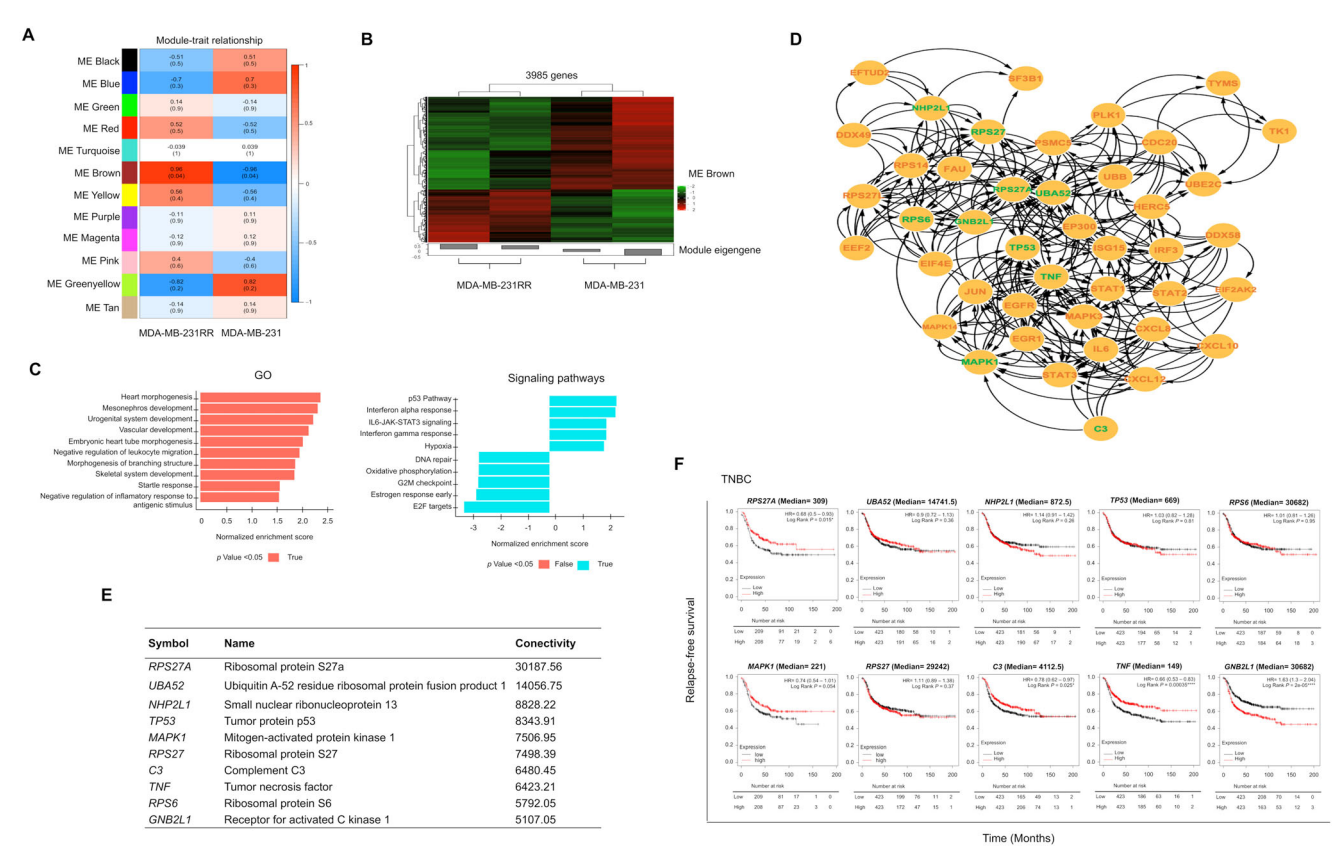


Figure 5. Weighted gene co-expression network and hub genes of MDA-MB-231RR cells and their clinical implication in TNBC subtypes of breast cancer. A) Correlation between the gene modules of transcriptome of MDA-MB-231RR cells. The connectivity of eigengenes analysis grouped into 12 modules is shown. B) Heat map that represents the correlation of 3985 genes of the brown module associated to radioresistant phenotype. Bar plots of gene set enrichment analysis for C)GO and enrichment signaling pathways of the brown module genes of MDA-MB-231RR cells. D) Interactome showing the top 10 hub genes and the co-expression network with 37 nodes. Gene names in green indicate the top 10 hub genes in the subnetwork based on the betweenness score. E) Table betweenness score of hub gene with higher degrees of connectivity from brown module of MDA-MB-231RR. F) Kaplan-Meier curves of RFS related to high versus low expression of hub genes in patients diagnosed with TNBC subtype and treated with radiotherapy. High or low expression levels according to > median or ≤ median expression levels of each gene. Curves were compared using a log-rank test *p ≤ 0.01, ***p ≤ 0.001. Rpm, reads per million.

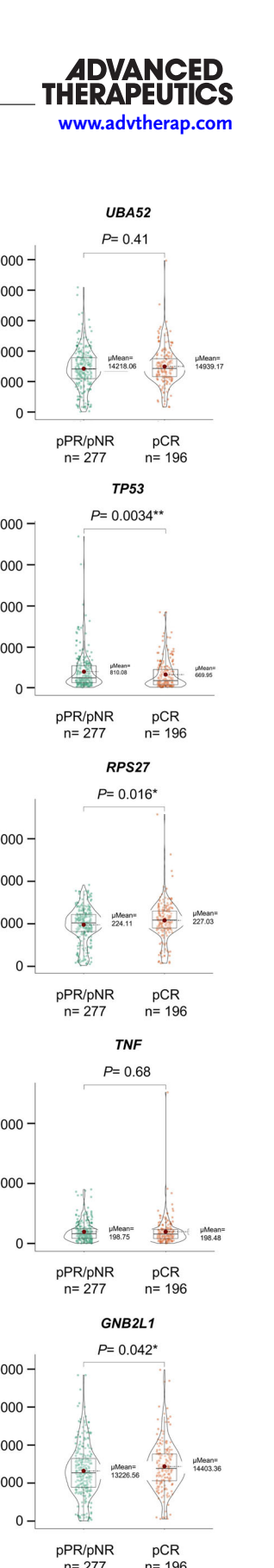
Genes were also associated to up-regulation of androgen response, hypoxia, epithelial mesenchymal transition (EMT) and down-regulation of mTORC1 signaling, while they may restrict immune response and inflammatory response (Figure 4C). Genes were filtered based on betweenness score to construct the co-expression network and to identify the hub genes. A co-expression network with 37 nodes was identified (Figure 4D), highlighting top 10 hub genes with high level of connectivity, including RPS27A, UBA52, JUN, PTPN11, MAPK1, UGT1A6, SRC, RACK1, STAT1, and EGFR genes (Figure 4E).

Likewise, the analysis of GO and biological pathways of the genes from the brown module in MDA-MB-231RR cells showed enrichment in differentiation and immune response. Pathways analyses displayed the up-regulation of p53 pathway, signaling IL-6/JAK/STAT3 and hypoxia, and down-regulation of DNA repair, oxidative phosphorylation, G2 checkpoint, estrogen response, and E2F targets (Figure 5C). The gene co-expression network showed 37 nodes (Figure 5D) and the top 10 hub genes as RPS27A, UBA52, NHP2L1, TP53, MAPK1, RPS27, C3, TNF, RPS6, and RACK1 (Figure 5E). Interestingly, RPS27A, UBA52, MAPK1, and RACK1 genes were commonly connected in the

co-expression networks both in MCF-7RR and MDA-MB-231RR cells suggesting that they might have a key functional role in the coordination of the molecular radioresistance network. Based on all these results obtained from the in vitro radioresistance model, the prognostic value of the top ten hub genes was evaluated in breast cancer patients diagnosed with luminal (Figure 4F) or TNBC (Figure 5F) tumors that received radiotherapy. The results from RFS analysis revealed that high levels of *STAT1* and low levels of *EGFR* were associated with worse outcomes in breast cancer patients with luminal tumor subtype after radiotherapy treatment (Figure 4F), while in TNBC patients, high levels of *GNB2L1* and low levels of *RPS27A*, *C3*, and *TNF* were associated with poor survival after radiotherapy (Figure 5F).

2.4. Genes Hub were Associated to Pathological Complete Response after Chemotherapy in Breast Cancer Patients

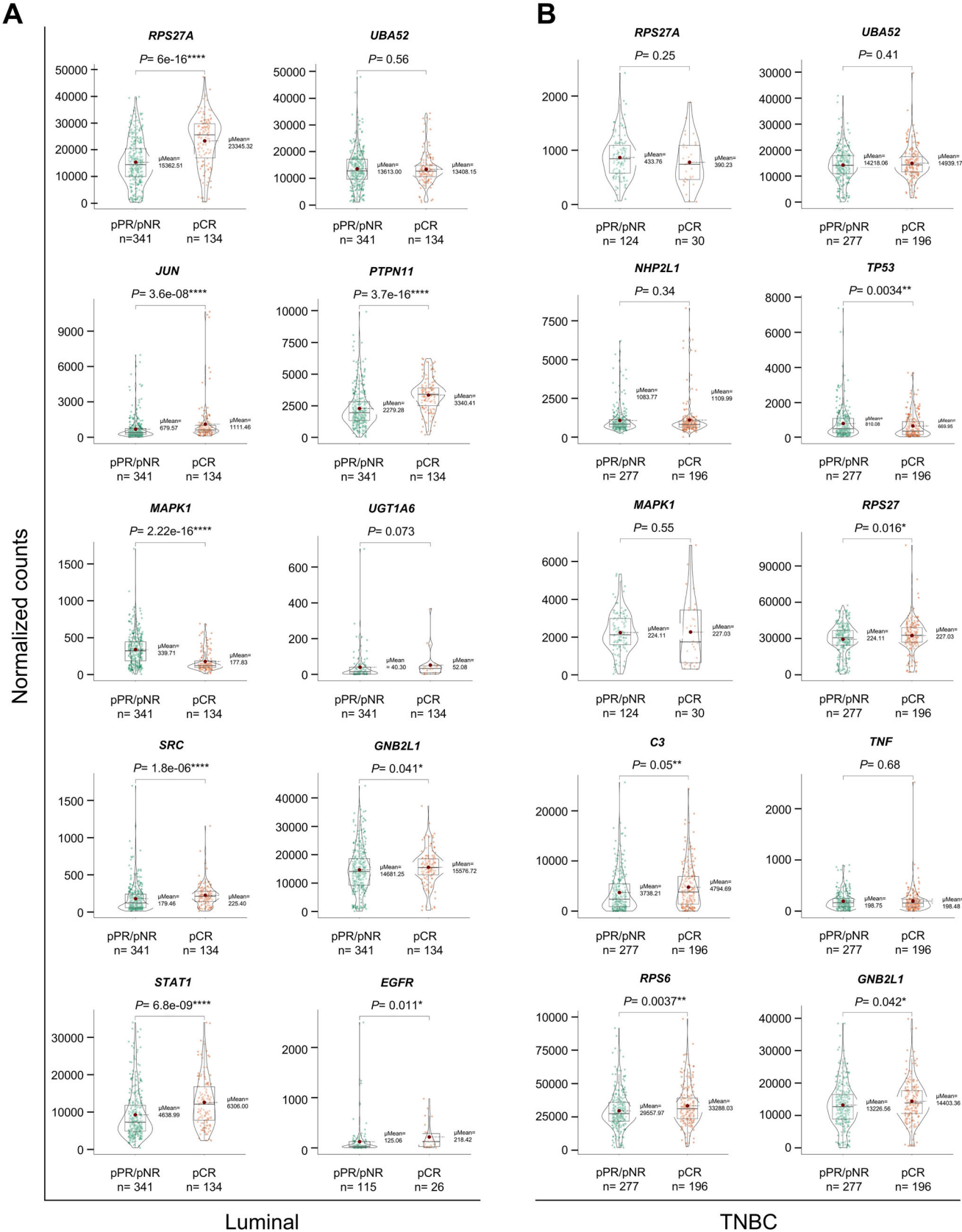
Based on previous observations in which radioresistant cells showed sensibility to chemotherapy agents and the hub genes may have possible related biological functions, the expression



23663987, 2024, 7, Downloaded

nelibrary.wiley.com/doi/10.1002/adtp.202300274 by Univer

Metropolitana, Wiley Online Library on [11/08/2025]. See the Terms





ADVANCEDTHERAPEUTICS

www.advtherap.com

level of hub genes in breast cancer patients with pathological complete response (pCR) or pathological partial/no response (pPR/pNR) after chemotherapy was evaluate. Interestingly, the results showed that patients with luminal tumors and pCR displayed overexpression of RPS27A, JUN, PTPN11, SRC, STAT1, and low expression of MAPK1 genes (Figure 6A). Overexpression of STAT1 gene was also associated to radioresistance in luminal tumors (Figure 4F) suggesting that STAT1 could play a role in the modulation of differential response to radio and chemotherapy. In TNBC, the results were also fascinating, low expression of TP53 and overexpression of C3 and RPS6 genes were associated with pCR (Figure 6B). C3 overexpression was also related with better outcome after radiotherapy in TNBC patients (Figure 5F). All these results indicate that transcriptomic modulation to evade the effectiveness of radiation treatment could activate pathways to favor the efficacy of chemotherapy. Our work suggests that after radiotherapy failure it may be important to evaluate different combinations of chemotherapy agents according to the expression of genes associate to radioresistance, including STAT1 gene in luminal subtypes and TP53, C3, and RPS6 genes for TNBC subtypes.

3. Discussion

Resistance to radiation reduces the effectiveness of antitumor therapy leading to poor outcome for breast cancer treatment. Thus, unveiling genes and biological processes related to radioresistance of breast tumor subtypes may support the selection of the patients that may not benefit with radiation therapy. In this study, we identified genes associated to radioresistance that were also related to better chemo-response. Cross-resistance to chemo and radiotherapy has been extensively studied, however the collateral sensitivity to chemotherapy of the radioresistant cells is still unknown.

To explore the transcriptomic background of the radiationresistant breast cancer cells, isogenic models of acquired radioresistance were used. MCF-7RR and MDA-MB-231RR cell lines comprise a validated in vitro model that mimics the biological behavior of radiation-resistant luminal and radiationresistance TNBC.[17] RR cells showed a higher survival fraction compared to parental cell lines under radiation treatment evidencing radioresistant phenotype. Radiation resistance is the result of complex cellular mechanisms enabling the acquisition of hallmark capabilities of cancer cells to promote tumor growth and metastasis. MDA-MB-231RR cell line showed a significant increase in migration rate. It has been reported that the parental MDA-MB-231 cell line shows selective advantages of clonogenicity and migration, and is characterized by being highly aggressive and proliferative.^[22] In MDA-MB-231RR cells, the result of an adaptive process to radiotherapy was inclined to enhance cell migration, contrary to MCF-7 cells, which are not migratory cells. In MCF-7RR cells, it seems radioresistance could favor other biological condition as proliferation, survival, or evasion of apoptosis. $^{[23-25]}$

In this regard, we assess the response to chemotherapeutic agents commonly used in the treatment of breast cancer to determine whether phenotypic plasticity produced by radiation was enough to also escape from the cytotoxic effect of doxorubicin, cyclophosphamide, and docetaxel. Surprisingly, chemotherapy significantly decreased cell viability favoring the apoptosis rates in RR cells, suggesting that radioresistant breast cancer cells might develop collateral sensitivity to chemotherapy aimed to block DNA replication and microtubule-targeting agents. In relation to this finding, it has been reported that some chemotherapeutic drugs promote the effectiveness of radiation.^[26] Similarly, we suggested that radiotherapy might promote chemo-sensitivity. Interestingly, the sensitivity of MCF-7RR cells seems to be specific to doxorubicin, cyclophosphamide, and docetaxel, but not to cisplatin. MDA-MB-231RR cells were sensitive to doxorubicin, cyclophosphamide, and cisplatin, but not to docetaxel. Remarkably, cisplatin might be an alternative treatment additional to doxorubicin and cyclophosphamide for TNBC that develop radioresistance.

The process of acquired resistance to radiotherapy comprise global transcriptional changes.[27] We evaluated the transcriptome of the RR cells to identify DEGs relative to parental cells. DEGs in MCF-7RR were mainly enriched to favor apoptosis and survival processes. While, in MDA-MB-231RR cells, DEGs were principally associated with inflammatory and migration cell processes. These results were according to previous studies related to the evaluation of the radio-sensitivity pathways of breast tumors. [28] Several authors have demonstrated that inhibition of proteins that activate survival pathways in luminal breast tumors^[23] and inflammatory proteins in TNBC^[24] may enhance the cytotoxic effect of radiation promoting radio-sensitivity.^[28] Survival and cell death seem strongly related to control radioresistance in breast cancer luminal subtype, whilst immune pathways and migration processes are mostly related to radioresistance in TNBC tumors.[25,29]

Although MCF-7RR and MDA-MB-231RR cells share a biological radioresistance phenotype, transcriptomic signatures, and biological pathways differ markedly. We explored gene interconnections by constructing gene co-expression networks highly correlated to radioresistant phenotype. Highly interconnected genes in MCF-7RR cells were enriched for DNA repair and metabolic processes, while MDA-MB-231RR cells were highly related to immune response and cell differentiation. These results were similar to those obtained in the analysis of DEGs, suggesting that these biological pathways could play a role in the specific regulation of radioresistant phenotype in luminal and TNBC subtypes respectively.^[30-35] Regarding the top 10 hub genes identified in the gene co-expression networks, we highlighted classical oncogenes in cancer as JUN, STAT1, and EGFR genes in luminal breast cancer^[34–36] and RPS27A, MAPK1, C3, TNF, and GNB2L1 genes in TNBC tumors.[37–43] All these genes

Figure 6. Hub genes expression in luminal and TNBC tumors of breast cancer patients with pCR or pPR/pNR after chemotherapy. A) The box plots show the expression of hub genes identified in MCF-7RR cells (RPS27A, UBA52, JUN, PTPN11, MAPK1, UGT1A6, SRC, RACK1, STAT1 and EGFR) evaluated in patients with luminal tumors who reported pCR or pPR/pNR after chemotherapy treatment. B) The expression of hub genes identified in MDA-MB-231RR cells (RPS27A, UBA52, NHP2L1, TP53, MAPK1, RPS27, C3, TNF, RPS6, and GNB2L1) evaluated in patients with TNBC tumors who reported pCR or pPR/pNR after chemotherapy treatment. ***** $p \le 0.0001$, ** $p \le 0.000$

ADVANCED SCIENCE NEWS

www.advancedsciencenews.com

ADVANCEDTHERAPEUTICS

www.advtherap.com

showed prognostic value in breast cancer patients submitted to radiotherapy. JUN and EGFR have not been reported in breast cancer radioresistance, however STAT1 is one of the better studied genes in the regulation of radiation response in cancer.[35] Interestingly, STAT1 in luminal tumors and C3 in TNBC were also associated with pCR after chemotherapy, which suggested that these genes might activate signaling that converge in antagonist pathways to radioresistance and chemosensitivity.[44,45] All these hypotheses must be deciphered by functional analysis. In addition, loss of expression of MAPK1 and up-regulation of RPS27A, IUN, PTPN11, SRC, and STAT1 in luminal breast tumors, and loss of expression of TP53 and overexpression of C3 and RPS6 genes in TNBC could be biomarkers for pCR after chemotherapy. It is relevant that MAPK expression decreased in RR cells as a common factor, however only in the luminal breast tumors was associated with pCR. Proteins coding by hub genes have been reported in the regulation of response to chemotherapy in breast cancer.[39-40,42-43,46-48] Our results revealed hub genes highly interconnected in biological networks related to radiation resistant phenotype in luminal and TNBC subtypes, some genes also play a role as prognostic biomarkers.

4. Conclusion

This study revealed DEGs and hub genes highly interconnected in the biological networks related to radioresistant phenotype that could conditioning the better response to chemotherapy. Radioresistant luminal breast cancer cells could favor survival pathways and evasion of apoptosis; while radioresistant TNBC subtype could promote pathways related to immune response, migration and cell differentiation. Clinically, the differential expression of EGFR, STAT1, JUN, HERC5 and CCL5 gene in luminal tumors, and RPS27A, GNB2L1, MAPK1, and CEACAM1 genes in TNBC were associated to prognosis of patients treated with radiotherapy. This work demonstrates that radioresistance pathways might converge to develop collateral chemo-sensitivity in breast cancer. All these findings provide new biomarkers for response to chemotherapy after radiotherapy relapsed.

5. Experimental Section

Cell Lines: Human breast cancer cell line MCF-7 and MDA-MB-231 were obtained from ATCC (# HTB-22 and HTB-26). MCF-7, MCF-7RR, MDA-MB-231, and MDA-MB-231RR cell lines were routinely cultured in Dulbecco Modified Eagle Medium (DMEM) (Gibco) supplemented with 10% fetal bovine serum and penicillin and streptomycin at 37 °C in a 5% $\rm CO_2$ atmosphere.

Establishment of Radioresistant Breast Cancer Cells: MCF-7RR and MDA-MB-231RR breast cancer cells were established from the parental MCF-7 and MDA-MB-231 cells lines as was described above by.^[17]

Clonogenic Assay: Clonogenic assays were performed as described above.^[18] Briefly, parental and RR cells were seeded in T-25 flasks and irradiated with 4 Gy of ionizing radiation as a lethal median dose.^[17] After 24 h, cells were harvested, counted, and seeded at 1000 cells per well in the 6-well plates. Cells were growing for 10 to 12 days. The surviving fraction (SF) was calculated as described.^[18]

Cell Migration: Cell migration was determined by real-time cell analysis migration assay with xCELLigence system (CIM- 12-well plates). A total of 6×10^4 parental or RR cells were seeded in the upper chamber in each well of the plates in serum-free media. Fresh DMEM was added to each

well of the lower chamber and the impedance value of the cells were analyzed for 72 h and expressed as a CI value.

Cytotoxicity Assay: Parental and RR cells were seeded at 1×10^4 cells/well in 96-well culture plates and were exposed to 2, 4, 6, 8, and $10\,\mu\text{M}$ of doxorubicin (Sigma-Aldrich; St. Louis, MO, USA); 20, 25, 30, 35, and 40 mM of cyclophosphamide (Sigma-Aldrich; St. Louis, MO, USA) or 5, 10, 20, 50 and 100 μM of docetaxel (Enzo Life Sciences; Farmingdale, NY, USA) for 24 h. Parental and RR cells were seeded at 1×10^6 cells/well in 6-well culture plates and were irradiated with 2, 4, 6, 8, and 10 Gy of ionizing radiation. After 24 h of radiation, cells were detached, and seeded at 1×10^4 cells/well in 96-well culture plates for 24 h to evaluated cytotoxicity. After all treatment, cytotoxicity was evaluated by MTT assay (Merck, USA) following the manufacturer's instructions.

Apoptosis Assay: Parental and RR cells were exposed to doxorubicin (10 μ M), cyclophosphamide (40 mM), docetaxel (50 μ M) or cisplatin (25 μ g/mL) as a positive control by 24 h. After that, apoptotic cells were analyzed by annexin V assay (Annexin-V-FLUOS staining kit; Roche) and flow cytometry according to manufacturer's instructions. Annexin V positive cells were identified as early apoptotic cells, annexin V and propidium iodide (PI) positive cells were considered as late-stage apoptotic cells, whereas PI-positive cells as necrotic cells.

Microarray-Based Gene Expression Analysis: Total RNA was obtained from parental and MCF-7RR and MDA-MB-231RR cells. Equimolar concentrations of total RNA from 3 independent clones were mixed and hybridized to an Affymetrix st1 array for the analysis of 29 834 genes. The gene expression profiles of each group were derived from two independent experiments. The arrays were analyzed by Transcriptome Analysis Console (TAC) through a not supervised analysis. DEGs was obtained according to statistical significance by ANOVA (p < 0.05). Up-regulated and down-regulated genes were considered from a fold change of >2.0 and <2.0 respectively. Accession number to Genbank (GEO accession number: GSE210306).

Co-Expression Network Construction and Module Eigengenes Detection: Gene co-expression networks were obtained from the weighted and signed correlation matrices following the protocols of WGCNA. The software R (version 4.0.2) with the "wgcna" R package (version 1.70-3) was used for WGCNA. A blockwiseModules R function was implemented using the following parameters: power = 20, minModuleSize = 30, deepSplit = 0, neworkType = "signed." Briefly, Pearson correlation coefficients were calculated for all pair-wise comparisons of the genes across all samples. The resulting Pearson correlation matrix was transformed into a matrix of connection strengths by a power function [connection strength = (0.5 + 0.5*correlation)], which resulted in a weighted network. Topological overlap measure (TOM), a biologically meaningful measure of node similarity was then calculated using a dynamic tree-cutting algorithm. Genes were hierarchically clustered using 1-TOM as the distance measure. Modules were determined by choosing a height cutoff 0.90 for the resulting dendrogram. Highly similar modules were identified by clustering and merged together. The module eigengene (ME) corresponds to the first principal component of a given module. Correlations between ME and radioresistance and chemosensitivity were calculated to identify a module that was highly related to radioresistance and chemosensitivity in both MCF-7RR and MDA-MB-231RR cells.

Functional Annotation of Co-Expression Modules: The genes of the brown modules related to radioresistance and chemosensitivity in both MCF-7RR and MDA-MB-231RR cell lines were used to conduct functional enrichment analysis. The GO and Kyoto Encyclopedia of Genes and Genomes (KEGG) pathway enrichment analyses were performed with the "fgsa" R package (version 1.14.0). If there were more than 10 GO annotation and pathway enrichments, only the top 10 terms with a p < 0.05 were extracted.

Identification of Hub Genes and Construction of PPI Network: A network of screening functions based on gene significance and module membership was used to screen hub-genes using Cytoscape software (version 3.8.2). Betweenness centrality of nodes was calculated using the "cyto-Hubba" tool in Cytoscape. Colors of the top 10% of the network were adjusted based on centrality value (green = top 10 hub-genes).

23663987, 2024, 7, Downloaded from https://advancec

onlinelibrary.wiley.com/doi/10.1002/adtp.202300274 by Universidad Autonoma Metropolitana, Wiley Online Library on [11/08/2025]. See the Terms

and-conditions) on Wiley Online Library for rules of use; OA articles are governed by the applicable Creative Commons

www.advtherap.com

The Cancer Genome Atlas Data Analysis: The predictive value of the hub genes was evaluated in a cohort of breast cancer patients received primarily radiotherapy or additional radiotherapy after surgery. The relapsefree survival (RFS) was assessed by the Kaplan-Meier method and the Log-Rank test. The expression of hub genes was associated to pCR or pPR/pNR in a second cohort of breast cancer patients received primarily chemotherapy. RNA Seq data were used for all assays. The expression levels of genes were referred to as reads per million (RPM).

Statistical Analysis: All results were derived from two or three independent experiments which were plotted as mean \pm standard deviation (SD). The comparison between the groups was performed using ANOVA test. For all analyses, statistically significant $p \leq 0.05$ values. Wilcoxon test was used for expression genes between tumors. All statistical analyses were performed using the statistical software package SPSS 17.0.

Supporting Information

Supporting Information is available from the Wiley Online Library or from the author.

Acknowledgements

Isidro X. Perez-Añorve is recipient of CONAHCyT fellowship (#A1-S-21433). Mauricio Flores-Fortis is recipient of CONAHCyT fellowship (#472137). The authors are grateful to Dr. Christian Adame (Hospital "20 de Noviembre" ISSSTE, México) and M.Sc. Oscar Angeles (Centro Medico Nacional 'Siglo XXI', Mexico) for optimizing the radiotherapy dose for all of the experimental analysis. This work was partially supported by Programa Especial de Apoyo a la Investigación-Rectoría Universidad Autónoma Metropolitana [Number: 47301023]. Availability of date and materials: Reference data for genomic analysis of global gene expression of the cell lines MCF-7RR and MDA-MB-231RR are available at: GenBank accession number (GEO accession number: GSE210306).

Conflict of Interest

The authors declare no conflict of interest.

Author Contributions

I.X.P.A., M.F.F., O.D.M.H., and E.A.O. conceived the study concept and design and wrote the manuscript. I.X.P.A., M.F.F., C.C.P.M., D.O.B., D.A.L.H., R.B.M., and E.A.O. development of methodology. I.X.P.A., M.F.F., C.C.P.M., D.O.B., D.A.L.H., E.O.G., R.B.M., and E.A.O. acquired the data. I.X.P.A., M.F.F., C.C.P.M., O.D.M.H., C.H.G.R., E.S.R., M.C.S., N.V.S., and E.A.O. analyzed and interpreted the data. I.X.P.A., M.F.F., C.C.P.M., O.D.M.H., D.O.B., D.A.L.H., E.O.G., C.H.G.R., E.S.R., N.V.S., and E.A.O. wrote, reviewed, and drafted the manuscript. O.D.M.H., C.H.G.R., E.S.R. M.C.S., N.V.S., and E.A.O. support of administrative, technical, and material. I.X.P.A., O.D.M.H., C.H.G.R. E.S.R., and E.A.O. supervised the study. All authors read and approved the final manuscript.

Data Availability Statement

The data that support the findings of this study are available in the supplementary material of this article.

Keywords

breast cancer, chemosensitivity, hub-genes, radioresistance, transcriptome

Received: July 29, 2023 Revised: February 27, 2024 Published online: June 6, 2024

- J. Haussmann, S. Corradini, C. Nestle-Kraemling, E. Bölke, F. J. D. Njanang, B. Tamaskovics, K. Orth, E. Ruckhaeberle, T. Fehm, S. Mohrmann, I. Simiantonakis, W. Budach, C. Matuschek, *Radiat. Oncol.* 2020, 15, 71.
- [2] C. Hennequin, I. Barillot, D. Azria, Y. Belkacémi, M. Bollet, B. Chauvet, D. Cowen, B. Cutuli, A. Fourquet, J. M. Hannoun-Lévi, M. Leblanc, M. A. Mahé, Cancer Radiother. 2016, 20, S139.
- [3] Y. S. Kwon, M. G. Lee, J. Baek, N. Y. Kim, H. Jang, S. Kim, Biochem. Pharmacol. 2021, 192, 114718.
- [4] C. Galeaz, C. Totis, A. Bisio, Front. Oncol. 2021, 11, 662840.
- [5] X. Lin, D. Kong, Z. S. Chen, Front. Pharmacol. 2022, 13, 904063.
- [6] C. Lagadec, E. Vlashi, Della Donna L, C. Dekmezian, F. Pajonk, Stem Cells 2012, 30, 833.
- [7] N. Jabbari, E. Akbariazar, M. Feqhhi, R. Rahbarghazi, J. Rezaie, J. Cell. Physiol. 2020, 235, 6345.
- [8] M. Belli, M. A. Tabocchini, Int. J. Mol. Sci. 2020, 21, 5993.
- [9] M. Katoh, Int. J. Oncol. 2017, 51, 1357.
- [10] L. Cassetta, S. Fragkogianni, A. H. Sims, A. Swierczak, L. M. Forrester, H. Zhang, D. Y. H. Soong, T. Cotechini, P. Anur, E. Y. Lin, A. Fidanza, M. Lopez-Yrigoyen, M. R. Millar, A. Urman, Z. Ai, P. T. Spellman, E. S. Hwang, J. M. Dixon, L. Wiechmann, L. M. Coussens, H. O. Smith, J. W. Pollard, *Cancer Cell* 2019, 35, 588. e10.
- [11] G. Deblois, S. A. M. Tonekaboni, G. Grillo, C. Martinez, Y. I. Kao, F. Tai, I. Ettayebi, A. M. Fortier, P. Savage, A. N. Fedor, X. Liu, P. Guilhamon, E. Lima-Fernandes, A. Murison, H. Kuasne, W. Ba-Alawi, D. W. Cescon, C. H. Arrowsmith, D. D. De Carvalho, B. Haibe-Kains, J. W. Locasale, M. Park, M. Lupien, Cancer Discov. 2020, 10, 1312.
- [12] O. Kaidar-Person, C. Lai, A. Kuten, Y. Belkacemi, Breast 2013, 22, 411.
- [13] S. Lev, Biochem. Soc. Trans. 2020, 48, 657.
- [14] N. N. Khodarev, B. Roizman, R. R. Weichselbaum, Clin. Cancer Res. 2012, 18, 3015.
- [15] Y. Nakayama, K. Mimura, T. Tamaki, K. Shiraishi, L. F. Kua, V. Koh, M. Ohmori, A. Kimura, S. Inoue, H. Okayama, Y. Suzuki, T. Nakazawa, D. Ichikawa, K. Kono, *Int. J. Oncol.* 2019, 54, 2030.
- [16] A. L. Hein, M. M. Ouellette, Y. Yan, Int. J. Oncol. 2014, 45, 1813.
- [17] I. X. Perez-Añorve, C. H. Gonzalez-De la Rosa, E. Soto-Reyes, F. O. Beltran-Anaya, O. Del Moral-Hernandez, M. Salgado-Albarran, O. Angeles-Zaragoza, J. A. Gonzalez-Barrios, D. A. Landero-Huerta, M. Chavez-Saldaña, A. Garcia-Carranca, N. Villegas-Sepulveda, E. Arechaga-Ocampo, Mol. Oncol. 2019, 13, 1249.
- [18] N. A. Franken, H. M. Rodermond, J. Stap, J. Haveman, C. van Bree, Nat. Protoc. 2006, 1, 2315.
- [19] L. Luzhna, O. Kovalchuk, Biochem. Biophys. Res. Commun. 2010, 392,
- [20] A. Pavlopoulou, Y. Oktay, K. Vougas, M. Louka, C. E. Vorgias, A. G. Georgakilas, Cancer Lett. 2016, 380, 485.
- [21] D. Trokic, G. Marosevic, V. Simeunovic, S. Lekic, B. Babic, Z. Gojkovic, JBUON 2021, 26, 466.
- [22] M. Kheirandish-Rostami, M. H. Roudkenar, A. Jahanian-Najafabadi, K. Tomita, Y. Kuwahara, T. Sato, A. M. Roushandeh, *Life Sci.* 2020, 244, 117339
- [23] Y. Y. Qu, S. L. Hu, X. Y. Xu, R. Z. Wang, H. Y. Yu, J. Y. Xu, L. Chen, G. L. Dong, PLoS One 2013, 8, e70727.
- [24] K. X. Zhou, L. H. Xie, X. Peng, Q. M. Guo, Q. Y. Wu, W. H. Wang, G. L. Zhang, J. F. Wu, G. J. Zhang, C. W. Du, Cancer Lett. 2018, 418, 196.
- [25] K. Y. Kim, A. Baek, Y. S. Park, M. Y. Park, J. H. Kim, J. S. Lim, M. S. Lee, S. R. Yoon, H. G. Lee, Y. Yoon, D. Y. Yoon, Y. Yang, *Oncol Rep.* 2009, 22, 1497.
- [26] M. R. Gill, K. A. Vallis, Chem. Soc. Rev. 2019, 48, 540.
- [27] S. de Mey, I. Dufait, M. De Ridder, Front Oncol. 2021, 11, 761901.
- [28] L. He, Y. Lv, Y. Song, B. Zhang, Cancer Manag. Res. 2019, 11, 5765.
- [29] M. Kim, H. Y. Choi, J. W. Woo, Y. R. Chung, S. Y. Park, Sci. Rep. 2021, 11, 18007.

ADVANCED SCIENCE NEWS

www.advancedsciencenews.com



www.advtherap.com

- [30] F. R. Greten, S. I. Grivennikov, Immunity. 2019, 51, 27.
- [31] H. Y. Liu, Y. Y. Liu, F. Yang, L. Zhang, F. L. Zhang, X. Hu, Z. M. Shao, D. Q. Li, Nucleic Acids Res. 2020, 48, 3638.
- [32] K. A. Brown, Nat. Rev. Endocrinol. 2021, 17, 350. s41574-021-00487-0.
- [33] Y. Yan, Z. Li, X. Xu, C. Chen, W. Wei, M. Fan, X. Chen, J. J. Li, Y. Wang, J. Huang, BMC Complement. Altern. Med. 2016, 16, 113.
- [34] G. M. Calaf, T. K. Hei, Int. J. Oncol. 2004, 25, 1859.
- [35] S. Liu, S. Imani, Y. Deng, J. L. Pathak, Q. Wen, Y. Chen, J. Wu, Onco. Targets Ther. 2020, 13, 6037.
- [36] L. S. Steelman, W. H. Chappell, S. M. Akula, S. L. Abrams, L. Cocco, L. Manzoli, S. Ratti, A. M. Martelli, G. Montalto, M. Cervello, M. Libra, S. Candido, J. A. McCubrey, Adv. Biol. Regul. 2020, 78, 100758.
- [37] H. Wang, J. Yu, L. Zhang, Y. Xiong, S. Chen, H. Xing, Z. Tian, K. Tang, H. Wei, Q. Rao, M. Wang, J. Wang, Biochem. Biophys. Res. Commun. 2014, 446, 1204.
- [38] A. López-Cortés, A. Cabrera-Andrade, J. M. Vázquez-Naya, A. Pazos, H. Gonzáles-Díaz, C. Paz-Y-Miño, S. Guerrero, Y. Pérez-Castillo, E. Tejera, C. R. Munteanu, Sci. Rep. 2020, 10, 8515.
- [39] T. Hu, R. Zhou, Y. Zhao, G. Wu, Sci. Rep. 2016, 6, 33376.
- [40] W. Si, J. Shen, C. Du, D. Chen, X. Gu, C. Li, M. Yao, J. Pan, J. Cheng, D. Jiang, L. Xu, C. Bao, P. Fu, W. Fan, Cell Death Differ. 2018, 25, 406.

- [41] C. Shu, H. Zha, H. Long, X. Wang, F. Yang, J. Gao, C. Hu, L. Zhou, B. Guo, B. Zhu, J. Exp. Clin. Cancer Res. 2020, 39, 11.
- [42] Z. Zhang, G. Lin, Y. Yan, X. Li, Y. Hu, J. Wang, B. Yin, Y. Wu, Z. Li, X. P. Yang, Oncogene 2018, 37, 3456.
- [43] Y. Fan, W. Si, W. Ji, Z. Wang, Z. Gao, R. Tian, W. Song, H. Zhang, R. Niu, F. Zhang, Breast Cancer Res. 2019, 21, 66.
- [44] M. Ye, Y. Chen, J. Liu, J. Tian, X. Wang, K. L. Fok, J. Shi, H. Chen, Cell Proliferation 2022, 55, e13226.
- [45] S. R. Chan, W. Vermi, J. Luo, L. Lucini, C. Rickert, A. M. Fowler, S. Lonardi, C. Arthur, L. J. Young, D. E. Levy, M. J. Welch, R. D. Cardiff, R. D. Schreiber, *Breast Cancer Res.* 2012, 14, R16.
- [46] M. E. Legrier, I. Bièche, J. Gaston, A. Beurdeley, V. Yvonnet, O. Déas, A. Thuleau, S. Château-Joubert, J. L. Servely, S. Vacher, M. Lassalle, S. Depil, G. C. Tucker, J. J. Fontaine, M. F. Poupon, S. Roman-Roman, J. G. Judde, D. Decaudin, S. Cairo, E. Marangoni, *Br. J. Cancer* 2016, 114, 177.
- [47] G. Yang-Kolodji, S. M. Mumenthaler, A. Mehta, L. Ji, D. Tripathy, Biomarkers 2015, 20, 313.
- [48] H. Chen, S. Libring, K. V. Ruddraraju, J. Miao, L. Solorio, Z. Y. Zhang, M. K. Wendt, Oncogene 2020, 39, 7166.